

A novel fatty acid-binding protein (FABP) gene resulting from tandem gene duplication in mammals: transcription in rat retina and testis

Rong-Zong Liu, Xiaodong Li, Roseline Godbout *

Department of Oncology, University of Alberta, Cross Cancer Institute, 11560 University Avenue, Edmonton, Alberta, Canada, T6G 1Z2

ARTICLE INFO

Article history:

Received 18 June 2008

Accepted 6 August 2008

Available online 27 September 2008

Keywords:

Fatty acid-binding protein

Multigene family

Gene duplication

Retina

Spermatogenesis

ABSTRACT

We have identified a new member of the *FABP* gene family, designated *FABP12*. *FABP12* has the same structure as other *FABP* genes and resides in a cluster with *FABP4/5/8/9* within 300,000 bp chromosomal region. *FABP12* orthologs are found in mammals, but not in the zebrafish or chicken genomes. We demonstrate that *FABP12* is expressed in rodent retina and testis, as well as in human retinoblastoma cell lines. *In situ* hybridization of adult rat retinal tissue indicates that *FABP12* mRNA is expressed in ganglion and inner nuclear layer cells. Analysis of adult rat testis reveals a pattern of expression that is different from that of the known testis *FABP* (*FABP9*) in the testicular germ cells, suggesting distinct roles for these two genes during mammalian spermatogenesis. We propose that *FABP12* arose as the result of tandem gene duplication, a mechanism that may have been instrumental to the expansion of the *FABP* family.

© 2008 Elsevier Inc. All rights reserved.

Introduction

Intracellular lipid-binding proteins (iLBPs) are a group of low molecular mass (~15 kDa) proteins that bind long chain fatty acids, retinoids or other hydrophobic ligands [1–3]. iLBPs that bind long chain fatty acids are called fatty acid-binding proteins (FABPs). To date, nine FABPs have been identified in mammals, with each showing specific tissue distribution patterns and ligand preference [4,5]. Although the amino acid sequence of different FABPs may vary by as much as 70%, the “ β -barrel” tertiary structure is strikingly similar among all FABP members. Fatty acid ligands are accommodated in the central cavity of the β -barrel, which dramatically increases their solubility in the aqueous cytoplasm, thus facilitating their movement to target sites where they exert their biological effect [1,2,6]. Although a number of *FABP* genes have been inactivated in the mouse genome [7–9], overlapping functions between the different members of the *FABP* family has prevented delineation of their precise role in the cell [5]. Proposed functions for FABPs include cellular uptake and transport of long-chain fatty acids, interaction with other transport proteins, regulation of gene transcription, and cellular protection [5,6,10,11].

The genes encoding FABPs are dispersed throughout the genome. The *FABP* gene structure is well-conserved, with each gene consisting of four exons separated by three introns of variable sizes [1,3]. In mammals, each *FABP* gene exists as a single functional copy in the genome, although pseudogenes have been identified for mouse *Fabp3* [12] and *Fabp5* [13]. In contrast, the zebrafish genome has duplicated functional genes for most FABPs, a possible consequence of chromo-

some or whole genome duplication followed by subfunctionalization of *FABP* gene members [14–18]. It has been postulated that the *iLBP* multigene family arose from a single ancestor gene by at least 14 gene duplications [19].

In this paper, we report the identification of a novel member of the *FABP* family, designated as *FABP12*, in rat, mouse and humans. *FABP12* resides in a tandem *FABP* gene cluster with members of the *FABP* sub-family IV and encodes a protein with the highest level of identity to members of this sub-family. There is no counterpart to *FABP12* in the chicken and zebrafish genomes. The mRNA distribution of this novel *FABP* gene in rat retina and testicular seminiferous epithelium suggests unique physiological roles in these mammalian tissues.

Results

Cloning of a novel *FABP* cDNA from rodents and humans

Four *FABP* genes have been mapped to the same region of human chromosome 8: *FABP4* (8q21), *FABP5* (8q21.13), *FABP8* (also known as *PMP2*, 8q21.3–8q22.1) and *FABP9* (8q21.13) [3]. A more detailed examination of this chromosomal region reveals that all four *FABP* genes cluster within a 300,000 bp region (Fig. 1). Interestingly, prediction programs have identified an additional gene with similarity to the myelin P2 gene (*FABP8*) at this locus (Gene name LOC646486). Comparison of the human chromosome 8 *FABP* gene cluster with the homologous regions of other mammalian species indicates that both the four *FABP* gene cluster and the predicted *FABP*-like gene are conserved (see Fig. 1 for comparison of human, rat and mouse). The predicted *FABP*-like gene, which we designate *FABP12*, corresponds to gene name RGD1565000 in rat and gene name 1700008G05Rik in mouse. ESTs corresponding to

* Corresponding author. Fax: +1 780 432 8892.

E-mail address: roseline@cancerboard.ab.ca (R. Godbout).

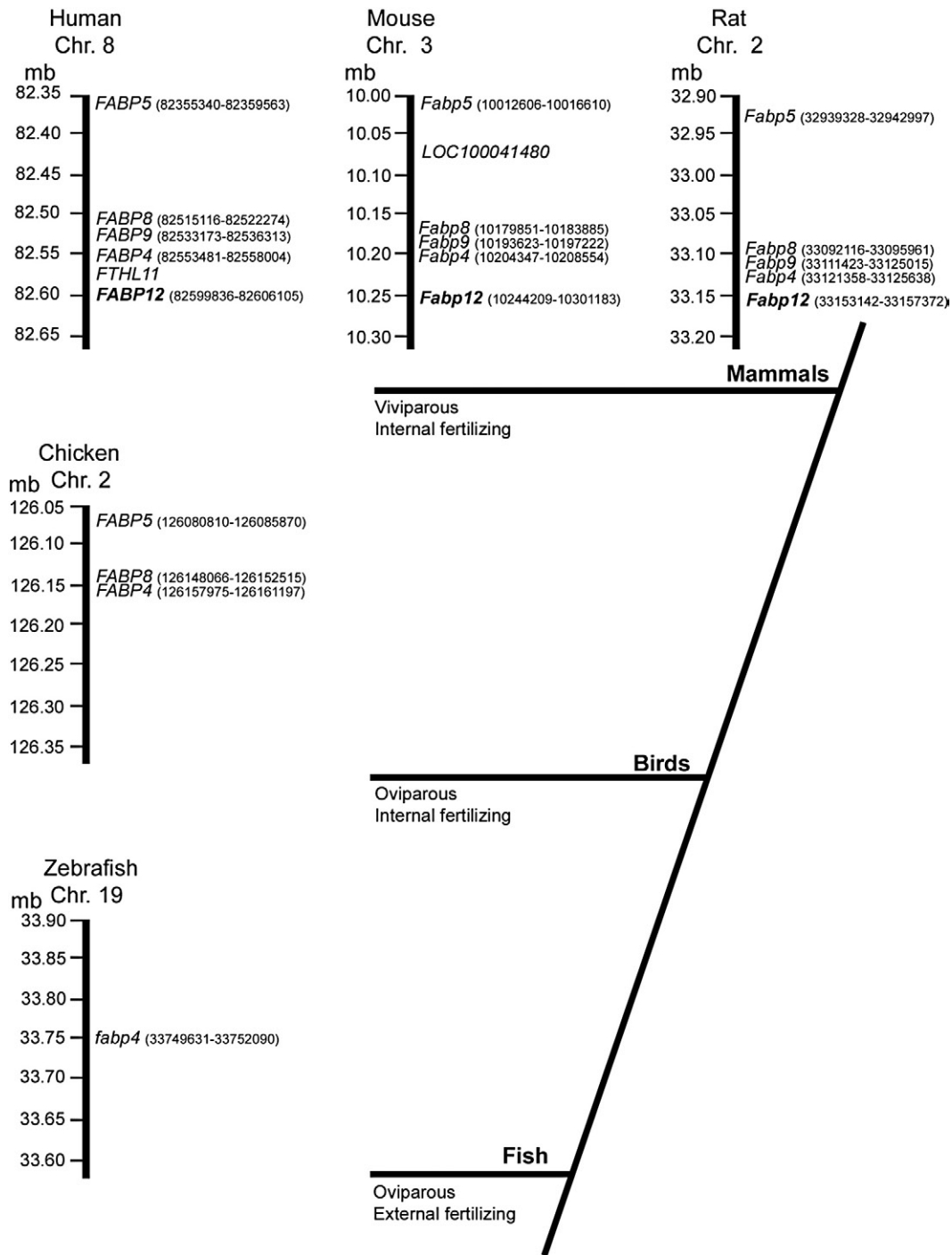


Fig. 1. Chromosomal localization of the *FABP12* gene in relation to an orthologous *FABP* gene cluster. Gene locations were defined based on the genomic DNA sequence annotation data obtained through Entrez Gene at the NCBI website (<http://www.ncbi.nlm.nih.gov/sites/entrez?db=gene&cmd>). The novel *FABP12* gene from human, mouse and rat is in bold. The orthologous clusters from chicken and zebrafish are also shown.

the predicted *FABP12* RNA sequence have been cloned from human, rat, and mouse eye and/or testis cDNA libraries (NCBI Unigene site – <http://www.ncbi.nlm.nih.gov/sites/entrez>).

To obtain the complete cDNA sequence of *FABP12*, we first generated the 3' end by 3' rapid amplification of cDNA ends (3' RACE). Gene-specific sense primers (s1 for rat, s6 for mouse, s7/s8 for human – Supplementary Table S1) were designed based on the genomic DNA sequence immediately upstream of the predicted start site of the coding sequence. Templates used for cDNA extension were RNAs isolated from adult retina (rat and mouse) and a human

retinoblastoma cell line (RB778). The complete 5' cDNA ends of rat and mouse *FABP12* were obtained by 5' RNA Ligase-Mediated RACE (5' RLM-RACE, Ambion INC). Nested antisense primers were designed based on the cDNA sequences generated from the 3' RACE products (as1/as2 for rat, as7/as8 for mouse – Supplementary Table S1). The sequences of four to six independent 3' and 5' RACE clones were aligned and combined to form the complete rat and mouse *FABP12* cDNA sequences. The human *FABP12* cDNA sequence included the entire open reading frame (ORF) but lacked the complete 5' UTR.

The rat and mouse *FABP12* cDNAs are 646 bp and 778 bp, respectively. Both the rat and mouse *FABP12* cDNA sequences have an ORF of 132 amino acids. Human *FABP12* cDNA has an ORF of 140 amino acids with the extra 8 amino acids located at the C-terminus. The predicted molecular masses of rat, mouse and human *FABP12* are 14.9, 14.8 and 15.6 kDa, respectively, with isoelectric points of 8.89, 8.15 and 7.93. Polyadenylation signals (AATAAA) are located 16–28 bp upstream of the polyadenylation sequences (Supplementary Fig. S1).

The predicted amino acid sequences of rat and mouse *FABP12* are 92% identical to each other and ~80% identical to that of human *FABP12* (Fig. 2). Identity to other members of the *FABP* family was considerably lower, with 47–66% identity to the subfamily IV members (*FABP3*, *FABP4*, *FABP5*, *FABP7*, *FABP8*, *FABP9*) as defined by Haunerland and Spener [5], 39–44% identity to fish *FABP11* (*FABP4*), ~27% to *FABP10*, and less than 25% identity to *FABP1*, *FABP2* and *FABP6*. The highest percent identity was to *FABP8* (60%–66%), followed by *FABP9* (53–58%). Three highly conserved residues in subfamily IV *FABPs* (Arg106, Arg126, Tyr128), shown to interact with the carboxyl group of fatty acid ligands [20], were also conserved in *FABP12* (Supplementary Fig. S1).

To determine the phylogenetic relationship between the newly identified mammalian *FABP12* and paralogous vertebrate *FABPs*, phylogenetic analysis was performed using CLUSTALX [21]. A bootstrap neighbor-joining phylogenetic tree (Fig. 3) was constructed with amino acid sequences of vertebrate *FABPs* retrieved from the NCBI website (www.ncbi.nlm.nih.gov/). The rat, mouse and human *FABP12* clustered with vertebrate *FABP4*, *FABP5*, *FABP8* and *FABP9* in a distinct clade of the tree with a bootstrap value of 1000/1000 (Fig. 3). It is noteworthy that this phylogenetic group consists of all five *FABP* genes clustered at the same chromosomal locus.

The gene structure of FABP12

The transcription start site of *Fabp12* was determined by 5'RLM-RACE, a technique designed to amplify cDNA from full-length capped mRNAs. A single product was identified in rat whereas two distinct products were found in mouse (Fig. 4). By sequencing of the 5'RLM-RACE clones, we mapped the transcription start sites of rat and mouse *Fabp12* to positions -48,772 and -1916, respectively, relative to the ATG start codon. Alignment of the complete rat and mouse *Fabp12* cDNA sequences with the corresponding genomic sequences indicates that the rat and mouse genes span 54,560 bp and 8308 bp, respectively (Fig. 5). Both rat and mouse *Fabp12* have five exons,

including a non-coding exon (Exon 0) in the 5' upstream region and four coding exons. Sequencing of the 5' cDNA ends of mouse *Fabp12* identified an alternatively splice variant lacking 158 nucleotides from the 3' end of Exon 0 (Supplementary Fig. S1 – highlighted sequence). The human *FABP12* gene also has four coding exons (Fig. 5), a structure common to all vertebrate *FABP* genes identified to date. As we did not isolate the 5' UTR of human *FABP12*, we are not able to tell whether it also contains a non-coding exon. The nucleotides at the splice sites of the exon–intron junctions of the rat, mouse and human *FABP12* genes all conformed to the GT-AG rule [22].

The FABP12 gene is phylogenetically restricted

The *FABP12* gene was identified in the genomes of rat, mouse and human where it is closely linked to four other *FABP* genes (*FABP4*, *FABP5*, *FABP8*, *FABP9*). *Fabp12* is contiguous to *Fabp4* in the rat and mouse genomes, and separated from *FABP4* by a single pseudogene *FTHL11* in the human genome (Fig. 1). Based on TBLASTN searches using the rat *Fabp12* amino acid sequence, *FABP12* orthologs are found in *Canis familiaris* (Gene name LOC487017, amino acid sequence identity 83%), *Equus caballus* (LOC100057343, 81%), *Pan troglodytes* (LOC748819, 80%) and *Macaca mulatta* (LOC706134, 78%). Orthologs of *FABP12* were not identified in the genomes of non-mammalian species. To confirm the absence of *FABP12* in non-mammalian genomes, we examined the regions of the chicken and zebrafish genomes harboring *FABP12* syntenic genes (Table 1). In chicken, the orthologous region was mapped to chromosome 2, which contains *FABP4*, *FABP5* and *FABP8*, but not *FABP9* and *FABP12* (Fig. 1, Table 1). In zebrafish, the paralogous locus was mapped to chromosome 19 which contains a single *FABP* gene, *fabp4* (also known as *fabp11a*). Interestingly, there is no evidence that the *FABPs* missing from the *FABP* cluster (*FABP9* and *FABP12* in the case of chicken; *FABP5*, *FABP8*, *FABP9* and *FABP12* in the case of zebrafish) are found anywhere else in their respective sequenced genomes.

Expression of FABP12 in retina and testes

To investigate the tissue-specific distribution pattern of *FABP12*, we analyzed mRNA expression in adult rat and mouse tissues by semi-quantitative RT-PCR using gene-specific primers (s1/as1 for rat and s6/as7 for mouse – see Supplementary Table S1). Abundant and specific PCR products were observed in adult rat/mouse retina and testis (Figs. 6A, C). Bands of lower intensity were also observed in

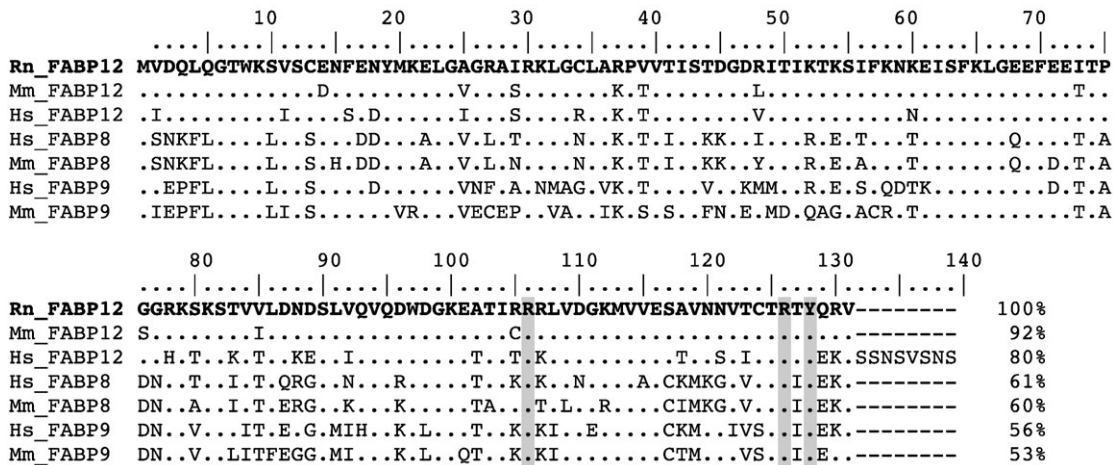


Fig. 2. Comparison of the amino acid sequences of the rodent and human *FABP12* with its two most highly related paralogs, *FABP8* and *FABP9*. The deduced amino acid sequences of the rat (GenBank accession no. EU733648), mouse (EU733649) and human (EU733650) *FABP12* were compared to the sequences of human and mouse *FABP8* (NP_002668, NP_002668) and *FABP9* (NP_001073995, NP_035728). Dots indicate amino acid identity. Dashes have been introduced to maximize alignment. The percentage amino acid sequence identity is indicated at the end of each sequence. The amino acid residues conserved in all subfamily IV *FABPs* and implicated in fatty acid ligand binding are highlighted in grey.

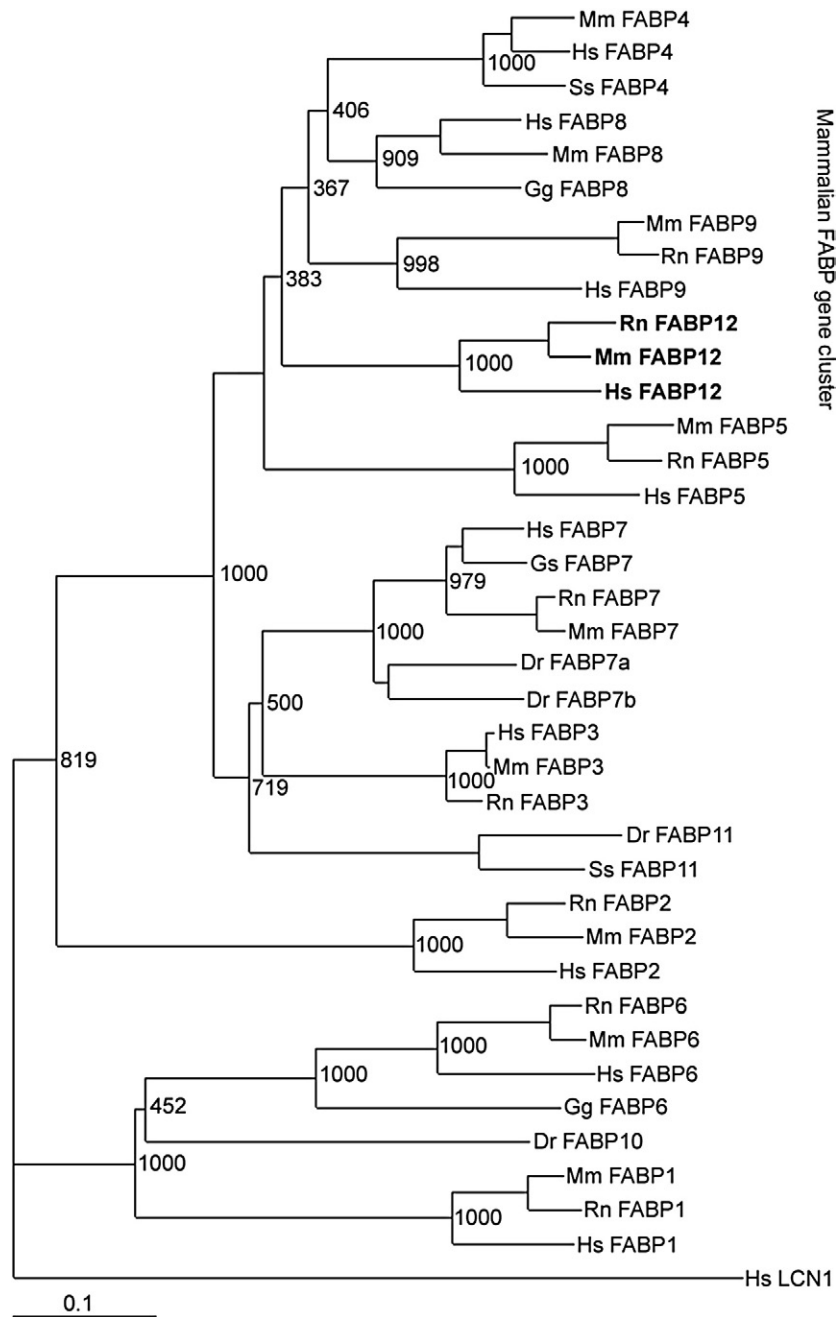


Fig. 3. Phylogenetic analysis of fatty acid binding proteins. The bootstrap neighbor-joining phylogenetic tree was constructed using CLUSTALX. The human lipocalin 1 protein sequence (LCN1, GenBank accession no. NP_002288) was used as an outgroup. The bootstrap values (based on number per 1000 replicates) are indicated on each node. Amino acid sequences used in this analysis include rat (Rn) Fabp12 (EU733648), Fabp9 (NP_074045), Fabp7 (NP_110459), Fabp6 (NP_058794), Fabp5 (NP_665885), Fabp3 (NP_077076), FABP2 (NP_037200), Fabp1 (NP_036688), mouse Fabp12 (733649), Fabp9 (NP_035728), Fabp8 (NP_002668), Fabp7 (NP_067247), Fabp6 (NP_032401), Fabp5 (NP_034764), FABP4 (NP_077717), Fabp3 (NP_034304), Fabp2 (NP_032006), Fabp1 (NP_059095), human (Hs) FABP12 (EU733650), FABP9 (NP_001073995), FABP8 (NP_002668), FABP7 (NP_001437), FABP6 (NP_001436), FABP5 (NP_001435), FABP4 (NP_001433), FABP3 (NP_004093), FABP2 (NP_000125), FABP1 (NP_001434), chicken FABP8 (XP_018309), FABP7 (NP_990639), FABP6 (XP_414486), zebrafish fabp7a (NP_571680), fabp7b (NP_999972), fabp10 (NP_694492), fabp11a (NP_001004682), Senegalese sole (Ss) fabp11 (CAM_58515). The distinct clade of the mammalian FABP gene cluster is highlighted in gray. The novel FABP12 sequence is in bold. Scale bar=0.1 substitutions per site.

adult rat cerebral cortex, kidney and epididymis, but not in any of the other tissues tested, including retina and brain of P1 (post-natal day 1) rat (Fig. 6B) and human fetal tissues (brain, retina, kidney, lung, heart, liver, stomach, gut and spinal cord) (data not shown). These data suggest that *FABP12* is associated with differentiated tissue functions.

The RNA expression patterns of the other four genes (*FABP4*, *FABP5*, *FABP8*, *FABP9*) in the *FABP* cluster were compared with that of *FABP12* by RT-PCR analysis. As shown in Figs. 6A and B, *Fabp4* and *Fabp5* were widely expressed in both adult and P1 rat tissues. *Fabp8* expression

showed a more restricted expression in adult brain and lung whereas *Fabp9* (testis *Fabp*) was only detected in adult testis and epididymis. The expression pattern of *Fabp12* was most similar to that of *Fabp9*, although *Fabp12* was also relatively abundant in the retina.

Next, we examined whether *FABP12* was expressed in retinoblastoma, a tumour of the retina that affects children. Of the nine retinoblastoma cell lines tested, *FABP12* RNA was detected in four (Fig. 6D). Whether expression of *FABP12* in retinoblastoma cells reflects their cell-of-origin or is a consequence of tumor formation and/or progression is not known at this time. As a positive control, primers

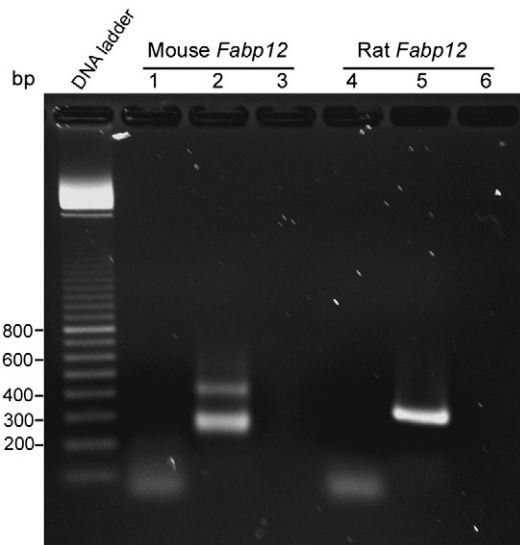


Fig. 4. 5' RLM-RACE products derived from capped and mature mouse and rat *FABP12* mRNA. Total RNA from adult mouse and rat retina was sequentially treated with calf intestinal alkaline phosphatase (CIP), tobacco acid pyrophosphatase (TAP) and then ligated to a designated RNA adapter. Following two rounds of nested PCR, two distinct PCR-amplified products were observed in mouse (lane 2) and a single product in rat (lane 5). The products of the first round of PCR are shown in lanes 1 and 4. PCR amplifications in the absence of template are shown in lanes 3 and 6. A 100 bp DNA ladder is shown on the left.

complementary to β -actin cDNA (*ACTB*) were used to generate PCR products from all rat, mouse and human tissues and cell lines tested.

In situ hybridization of *FABP12* in retina and testis

Tissue sections from adult rat retina were hybridized to antisense *Fabp12* transcripts labeled with digoxigenin (DIG)-11-UTP. A strong hybridization signal was detected in the ganglion cell layer as well as throughout the inner nuclear layer (Fig. 7). There was a complete absence of signal in the outer nuclear layer where the photoreceptors are located. Tissue sections hybridized to DIG-labeled *Fabp12* sense transcripts were completely negative (data not shown). The signal distribution in the inner nuclear layer suggests widespread expression in amacrine (located in the inner half of the inner nuclear layer) as well as in bipolar cells (located in the outer half of the inner nuclear layer). The presence of *Fabp12* transcripts in ganglion, amacrine and bipolar cells suggests a specific requirement for *Fabp12*-specific

ligands in neurons which are involved in transmission of the visual signal to the brain.

Previous work has suggested that *FABP9* (also termed *PERF15* or *T-FABP*) is the only *FABP* gene expressed in mammalian testicular germ cells [6,23]. Our RT-PCR data indicate that *Fabp12* is found at levels comparable to that of *Fabp9* in the adult rat testis. We therefore compared the cellular distribution patterns of *Fabp9* and *Fabp12* in adult rat testis. Consecutive tissue sections of adult rat testis were hybridized to either *Fabp9* or *Fabp12* riboprobes. As expected, both *Fabp9* and *Fabp12* transcripts were detected in the seminiferous tubules of adult rat testis. However, whereas *Fabp9* was detected in the first layer of spermatids and/or secondary layer of spermatocytes (presumably at the pachytene phase) in the seminiferous epithelium at all 14 stages (Fig. 8Ai) defined by Leblond and Clermont [24,25], *Fabp12* was only observed in spermatids at specific stages of the seminiferous epithelium cycle (Fig. 8Aii). As shown in Fig. 8Biv, *Fabp12*-specific hybridization signals were readily apparent in the first layer capped spermatids (step 7) at stage VII. In comparison, *Fabp9* transcripts were found in both pachytene spermatocytes and capped spermatids (Fig. 8Bi). As spermatids mature, they move toward the lumen side of the tubule. The *Fabp12* hybridization signal was observed in spermatids closer to the lumen at stage XII, whereas *Fabp9* transcripts were only detected in the pachytene spermatocytes (Fig. 8Bii,v,viii). *Fabp12* was undetectable at early stages of the seminiferous epithelium cycle (e.g. stage IV in Fig. 8Bvi). *FABP9* was widely expressed in step 4 spermatids at stage IV (Fig. 8Biii). Neither *Fabp9* nor *Fabp12* transcripts were detected in spermatogonia, first layer of spermatocytes and mature spermatozoa. Our *in situ* hybridization results indicate that while two different *FABP* genes are expressed in the seminiferous epithelium, their patterns of expression differ substantially. The dynamic distribution of *Fabp12* mRNA in the rat seminiferous epithelium indicates a unique role for this gene during spermatid development and maturation.

Discussion

Expansion of the FABP gene family in vertebrate genomes

To date, at least fifteen paralogous genes have been identified in the *iLBP* multigene family of mammals, including nine *FABP* genes, two cellular retinoic acid binding genes (*CRABP*) and four retinol binding protein genes (*RBP*). *iLBP* genes are found throughout the animal kingdom, from insects and amphibians to humans. However, the number and types of *iLBP* paralog differ among taxa. For example, *FABP10* is present in the genomes of fish, tetrapods and birds, but not in mammals [26–29], whereas *FABP9* is only found in mammalian

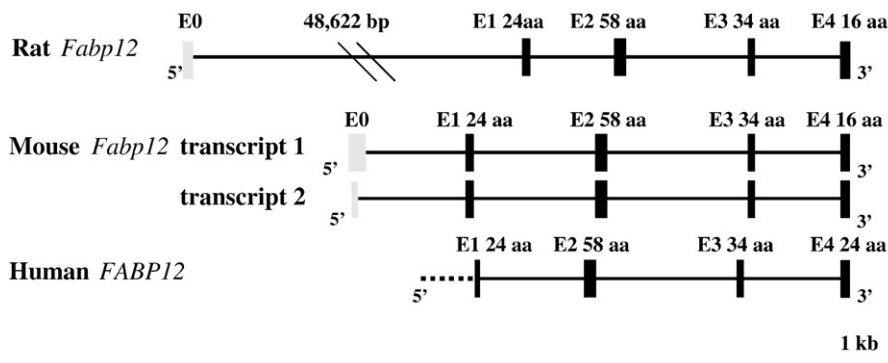


Fig. 5. Comparison of the exon/intron organization of the *FABP12* genes from rat, mouse and human. The positions of exons and introns were determined by blast alignment of cDNA sequences against genomic DNA sequences (GenBank accession nos. rat, NW_047623; mouse, NT_078380; human, NT_008183) (<http://www.ncbi.nlm.nih.gov>). Exons (E0, E1, E2, E3, E4) are shown as blocks and introns as lines. The number of amino acids encoded by each exon is shown above the blocks. The size of each exon and intron is approximately represented by the length of blocks and lines, respectively, except for intron 0 of rat *Fabp12*. The non-coding exons (E0) of the rat and mouse *Fabp12* are shown in gray. The region upstream of the human *FABP12* start codon is indicated by dots. Intron scale bar: 1000 basepairs (kb).

Table 1
Conserved synteny of a vertebrate *FABP* gene cluster

Gene	Human			Mouse			Rat			Chicken			Zebrafish		
	Chr.	Location (mb)		Chr.	Location (mb)		Chr.	Location (mb)		Chr.	Location (mb)		Chr.	Location (mb)	
		Start	Stop		Start	Stop		Start	Stop		Start	Stop		Start	Stop
<i>STMN2</i>	8q21.13	80.69	80.74	3	8.51	8.56	2q23	95.29	95.33	2	125.41	125.45	19	33.04	33.06
<i>HEY1</i>	8q21	80.84	80.84	3	8.66	8.67	2q23	95.17	95.18	2	125.47	125.55	19	33.07	33.08
<i>TPD52</i>	8q21	81.11	81.25	3	8.93	9.01	2q23	94.85	94.88	2	125.60	125.64	19	33.03	33.04
<i>ZNF704</i>	8q21.13	81.71	81.95	3	9.43	9.61	–	–	–	2	125.81	125.90	19	32.93	33.01
<i>PAG1</i>	8q21.13	82.04	82.19	3	9.69	9.83	2	87.53	87.66	2	125.92	126.00	19	32.89	32.92
<i>FABP5</i>	8q21.13	82.36	82.36	3	10.01	10.02	2	87.37	87.37	2	126.08	126.09	–	–	–
<i>FABP8</i>	8q21.3-q22.1	82.52	82.52	3	10.18	10.18	2q23	93.57	93.57	2	126.15	126.15	–	–	–
<i>FABP9</i>	8q21.13	82.53	82.54	3	10.19	10.20	2q23	93.55	93.55	–	–	–	–	–	–
<i>FABP4</i>	8q21	82.55	82.56	3	10.20	10.21	2q23	93.54	93.54	2	126.16	126.16	19	33.75	33.75
<i>FABP12</i>		82.60	82.61	3	10.24	10.30	2q23	93.50	93.51	–	–	–	–	–	–
<i>IMPA1</i>	8q21.13-q21.3	82.73	82.76	3	10.31	10.33	2q23	93.42	93.44	2	126.20	126.21	19	31.12	31.13
<i>SLC10A5</i>	8q21.13	82.77	82.77	3	10.33	10.34	2q23	93.41	93.41	–	–	–	–	–	–
<i>ZFAND1</i>	8q21.13	82.78	82.80	3	10.34	10.35	2	93.40	93.41	2	126.21	126.22	–	–	–
<i>CHMP4C</i>	8q21.13	82.81	82.83	3	10.37	10.39	2q23	93.33	93.38	2	126.22	126.24	–	–	–
<i>SNX16</i>	8q21.13	82.87	82.92	3	10.42	10.44	2q23	93.28	93.30	2	126.24	126.26	–	–	–

genomes [30, 31]. We previously showed that the fish genomes have more *iLBP* genes than mammals and birds [14–18], presumably as the result of whole genome duplication [32].

It is generally believed that the entire *iLBP* multigene family arose from a single ancestral gene through a series of gene duplications [3,19]; however, it's not clear how these duplications occurred. The novel *FABP12* gene described in this paper is solely found in mammalian genomes and is located within a gene cluster that contains four other *FABP* genes (*FABP4*, *FABP5*, *FABP8*, *FABP9*). Based on the following, we propose that appearance of *FABP12* in mammals is the result of relatively recent tandem gene duplication: (i) *FABP12* is tandemly arrayed with four *FABPs* included in the *iLBP* subfamily IV; (ii) *FABP12* shows the highest level of amino acid identity with that of the four *FABP* genes found in the same cluster; (iii) the expression profile of *FABP12* suggests close functional relationship with *FABP8* (both found in neuronal tissues) and *FABP9* (both found in testis), and (iv) phylogenetic analysis indicates that *FABP12* and other members of the cluster form a distinct clade suggesting a close phylogenetic relationship. Since neither *FABP9* nor *FABP12* orthologs are found in the chicken genome which contains a cluster of *FABP4*, *FABP5* and *FABP8*, the *FABP9* and *FABP12* genes must have arisen as the result of tandem duplication of the *FABP4*, *FABP5* or *FABP8* genes. Given the close genomic and functional relationship between *FABP12* and *FABP9*, one can further postulate a more recent tandem duplication for these two genes, with one being the progenitor of the other.

FABP3 and *FABP7* are also included in *iLBP* subfamily IV [4], even though they reside on different chromosomes from the *FABP4/5/8/9/12* cluster. It is interesting that both *fabp3* and *fabp4* (or *fabp11a*) have been mapped to chromosome 19 (LG 19) of zebrafish [33,34], albeit separated by ~10,000,000 bp. Synteny at the *fabp3* and *fabp4* (or *fabp11a*) loci in zebrafish have been shown to be conserved with synteny surrounding both the *FABP3* gene on human chromosome 1 and the *FABP4* gene on human chromosome 8 [33,34]. This suggests that the *FABP3* gene may also have arisen from tandem duplication followed by chromosomal re-arrangement resulting in diversification of chromosomal locations for *FABP3* and *FABP4* in mammals. Based on these data, we propose that the mammalian *FABP* subfamily IV may have arisen through sequential tandem duplications, and that this mechanism underlies expansion of the mammalian *FABP* gene family.

FABP12 expression in adult retina

The retina is rich in long-chain polyunsaturated fatty acids (PUFAs) which are important structural determinants of retinal cell membranes, and which, consequently, may play essential roles in retinal cellular differentiation, physiological function, survival and death [35].

As intracellular transporters of PUFAs, FABPs may serve as mediators of their physiological function, availability and access to intracellular targeted systems. Analysis of temporal and spatial FABP expression patterns in the developing and mature retina provides clues as to their possible functions in this tissue. To date, two other FABP proteins and/or mRNAs have been found in developing retina. In the developing chick embryo, retina FABP (R-FABP, a.k.a. B-FABP, BLBP or FABP7) is expressed in both neuronal and glial cell lineages [36,37]. E-FABP (or FABP5) localizes to the ganglion cells of the developing rat retina and is associated with axon development and regeneration [38]. Both FABP7 and FABP5 are enriched at early stages of retinal development [36–39]. In contrast, *FABP12* appears to be restricted to the adult retina. *Fabp12* transcripts are found in ganglion cells as well as in the inner nuclear layer which consists primarily of bipolar and amacrine cells, both of which are neuronal cells. Our results suggest that *FABP12* may be the most highly expressed FABP in adult retina.

Retinal ganglion cell death causes diseases of the optic nerve such as glaucoma [40]. Unsaturated fatty acids and ligands of PPAR γ have been shown to play a protective role in rat retinal ganglion cells preventing neurotoxicity caused by glutamate [41,42]. As FABPs transport fatty acids to the nucleus to target and activate PPARs or RXRs, which in turn regulate the expression of their target genes [10], *FABP12* may play a role in the regulation of genes required in adult retina. One possibility is that *FABP12* expression in adult ganglion cells plays a neuroprotective role in the retina, by binding and targeting fatty acids to PPARs/RXRs in the nucleus of ganglion cells, in turn regulating the expression of genes involved in neurotoxicity resistance. Such a neural cell maintenance mechanism may be crucial for retinal ganglion cell survival in adult mammalian species.

FABP9 and *FABP12* have distinct distribution patterns in testicular germ cells

Until now, mammalian *FABP9* was believed to be the only *FABP* gene expressed in mammalian testicular germ cells [6,23]. We show that a closely related paralog, *Fabp12*, is also expressed in rat testicular germ cells. Comparison of consecutive tissue sections hybridized to *Fabp9* and *Fabp12* riboprobes shows distinct distribution profiles in the seminiferous epithelium during spermatogenesis, with *Fabp9* expressed at earlier stages of spermatogenesis (pachytene spermatocytes to cap phase spermatids) and *Fabp12* expressed at later stages (cap phase spermatids to acrosome phase spermatids). As membrane remodeling is a key process in testicular germ cell development and maturation [43], and FABPs have been shown to bind specific fatty acids [4,44], it is not surprising that different FABPs would be required to fulfill the specific tasks related to fatty acid uptake, metabolism,

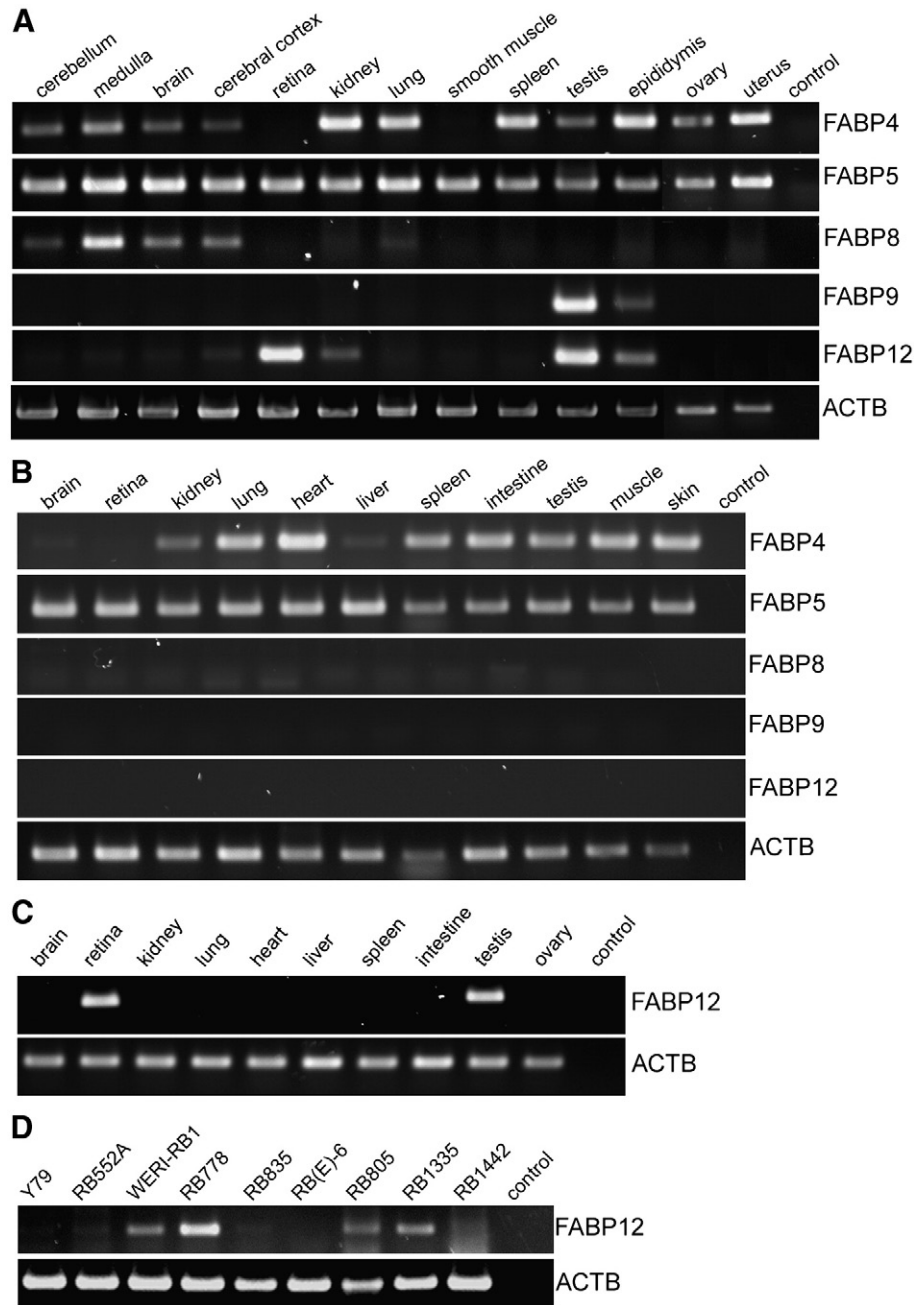


Fig. 6. Semi-quantitative analysis of *FABP12* transcripts and comparison with paralogous *FABPs* from the same cluster. RT-PCR products were generated using cDNA derived from total RNA extracted from the indicated tissues of adult rat (A), rat at post-natal day 1 (B), adult mouse (C) and human retinoblastoma cell lines (D). RT-PCR products corresponding to constitutively expressed β -actin were generated in all samples analysed. Omission of cDNA template from the RT-PCR reaction did not produce a signal (control).

membrane remodeling and nuclear function inherent to spermatogenesis. Grogan *et al.* [45] found complex changes in the fatty acid composition of mouse testicular germ cells as a function of developmental stage. For example, docosapentaenoic acid (DPA; 22:5n-6) increased from 2 to 20% of total fatty acids as preleptotene spermatocytes progressed to primary spermatocytes, round spermatids, and condensing spermatids, but decreased in mature spermatozoa. Arachidonic acid (AA; 20:4n-6) showed the reciprocal trend whereas docosahexanoic acid (DHA; 22:6n-3) showed little change during germ cell differentiation [45].

There are striking differences in the PUFA composition of testes amongst different species. For example, DHA is the most abundant fatty acid in human and monkey testes, whereas rat, hamster, rabbit and dog testes are especially rich in DPA, 22:5n-6 [46]. Interspecific

differences in sperm membrane lipid composition has been shown to be related to the variation of sperm tolerance to environmental stress among different species [47]. It is interesting that neither *fabp12* nor *fabp9* are present in oviparous (e.g. chicken) and external-fertilizing fish (e.g. zebrafish). Whether the products of these two *FABP* genes play special roles in germinal lipid metabolism and membrane remodeling during spermatogenesis in the viviparous and internal-fertilizing mammalian species awaits further investigation.

In summary, we have identified a new mammalian member of the *FABP* gene family that is abundantly expressed in retina and testis. The divergent spatial and temporal distribution of *FABP12* transcripts in these two tissues compared to that of their known paralogs suggest specific roles in the uptake, binding and distribution of fatty acids. We show that *FABP12* is part of a *FABP* cluster that contains four additional

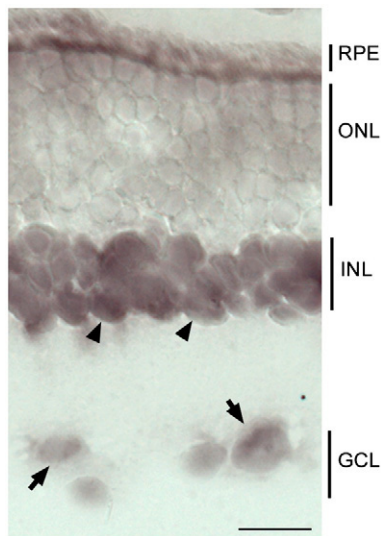


Fig. 7. *In situ* hybridization of adult rat retina tissue sections using a *FABP12* riboprobe. Sagittal tissue sections of adult rat retina were hybridized to DIG-11-UTP labeled *FABP12* cDNA specific antisense riboprobe. Hybridization signals were detected in cells of the ganglion layer (GCL, arrows) and the inner nuclear layer (INL, arrow heads), but not in cells of the outer nuclear layer (ONL) and retinal pigment epithelium (RPE). Cell layers are indicated by the vertical bars. Scale bar: 50 μ m.

FABP genes, all located within 300,000 bp of each other. We propose that *FABP12* arose in the mammalian genomes as a result of tandem gene duplication, and postulate that this mechanism may have played a prominent role in the expansion of the *FABP* gene family.

Materials and methods

Animals and Tissues

Fischer–Copenhagen F1 adult male and female rats and C57Bl/6 mice were handled and sacrificed according to protocols approved by the Canadian Council on Animal Care (CCAC). Tissues were either snap frozen in liquid nitrogen and preserved at -80°C for RNA extraction or fixed in 4% paraformaldehyde prior to embedding in OCT (Optimum Cutting Temperature) (Tissue-Tek, Miles Inc.).

cDNA cloning

The cDNA sequences of rat, mouse and human *FABP12* was obtained by 3' rapid amplification of cDNA ends (3'-RACE) and 5' RNA ligase mediated-RACE (5'RLM-RACE) using the FirstChoice RLM-RACE kit (Ambion Inc. USA). Briefly, total RNA was extracted from adult rat, adult mouse retina or the human retinoblastoma cell line RB778. For 3'-RACE, RNA was reverse-transcribed with a 3' adaptor primer (5'-GGCCACGCGTCTCGACTAGTACT₁₇-3') and PCR-amplified with gene specific sense primers (s1, s6, s7/s8, Supplementary Table S1) and the antisense primer complementary to the 3' adaptor. To clone the 5' cDNA ends, total RNA was first subjected to calf intestinal phosphatase to remove the 5' phosphate from uncapped RNAs, followed by tobacco acid pyrophosphatase to remove the cap from mRNAs. The resulting uncapped full-length mRNAs containing a 5' phosphate were ligated to a 5' RNA oligonucleotide adaptor using T4 RNA ligase. Random-primed reverse transcription and nested PCR using sense adaptor primers and antisense gene-specific primers (as1/as2 for rat, as7/as8 for mouse – see Supplementary Table S1) were then employed to amplify the 5' ends of the rat and mouse *Fabp12* transcripts. Both 3' RACE and 5' RLM-RACE products were purified from agarose gel with GENECLEAN SPIN kit (MP medicals LLC), cloned into pCRII-TOPO vector (Invitrogen) and sequenced. The transcription start sites of rat and mouse *Fabp12* were mapped by

aligning the 5' cDNA ends sequence with their corresponding genomic DNA sequences.

Phylogenetic analysis

Phylogenetic analysis of the rat, mouse and human *FABP12* and other vertebrate *FABPs* was performed using CLUSTALX [21]. A bootstrap neighbor-joining phylogenetic tree was constructed using the human lipocalin 1 protein sequence (LCN1, GenBank accession number: NP_002288) as an outgroup.

Semi-quantitative reverse transcription-polymerase chain reaction (RT-PCR)

Total RNA was extracted from tissues of rat (adult and P1), adult mouse and human retinoblastoma cell lines using Trizol reagent according to the manufacturer's protocol (Invitrogen). Five μ g of total RNA from each sample were used as the template for the synthesis of first strand cDNA by reverse transcriptase (SuperScript II, Invitrogen). The following oligonucleotides were used for PCR amplification (Supplementary Table S1): s1/as1 for rat *FABP12*, s6/as7 for mouse *FABP12*, s8/as9 for human *FABP12*, s5/as6 for rat *FABP4*, s4/as5 for rat *FABP5*, s3/as4 for rat *FABP8* and s2/as3 for rat *FABP9*. Optimum number of cycles (28 cycles for *FABP4*, *FABP5*, β -actin, and 30 cycles for *FABP8*, *FABP9* and *FABP12*) was determined for each pair of primers to allow semi-quantification of PCR products. PCR reactions were carried out in 20 μ L reaction volumes containing 0.5 U of *Taq* DNA polymerase, 1.5 mM MgCl_2 , 200 μ M of each dNTP, 0.25 μ M of each primer, and 1 μ L (out of a total of 50 μ L) cDNA template from the reverse transcription reaction. Following an initial denaturation step at 94°C for 2 min, the reaction was subjected to 28 or 30 cycles of amplification at 94°C for 30 s, 57°C for 30 s, 72°C for 30 s, with a final extension at 72°C for 7 min. Samples were size-fractionated in a 1% (w/v) agarose gel and the DNA visualized using ethidium bromide and UV light. β -actin amplified using s10/as12 (human) and s9/as11 (rat and mouse) primers served as the standard for amount of cDNA used for each reaction. Negative controls included all RT-PCR components with the exception of the cDNA template.

In situ hybridization of tissue sections

Plasmids containing rat *Fabp12* or rat *Fabp9* cDNA (entire open reading frame) were linearized with appropriate restriction enzymes and labeled with DIG-11-UTP by *in vitro* transcription using T7 or SP6 RNA polymerase (Roche) to yield sense or antisense riboprobes. Rat retina and testis were fixed in 4% PBS-buffered paraformaldehyde at 4°C , sequentially cryoprotected with 12%, 16% and 18% sucrose and embedded in OCT. Tissue sections (6–8 μ m thick) were incubated at 55°C for 4 h in pre-hybridization buffer containing 40% formamide, 10% dextran sulfate, $1\times$ Denhardt's solution, $4\times$ SSC, 10 mM DDT, 1 mg/mL yeast tRNA and 1 mg/mL heat-denatured herring testis DNA. Approximately 30 ng labeled riboprobe were heat-denatured and mixed with 100 μ L pre-hybridization mix and hybridized to tissue sections overnight at 55°C . Tissue sections were sequentially washed with 50% formamide in $2\times$ SSC followed by $2\times$ SSC. Slides were then incubated with alkaline-phosphatase (AP)-conjugated anti-DIG antibody overnight at room temperature in a humidified chamber. Hybridization signals were detected with 0.45% (v/v) NBT and 0.35% (v/v) BCIP in polyvinyl alcohol. In some cases, *Fabp12*-hybridized tissue sections were counterstained with methyl green, washed with 95% ethanol and mounted with xylene.

Acknowledgments

We would like to thank Elizabeth Monckton for preparing the rat retina and testis tissue sections. This project was supported by a

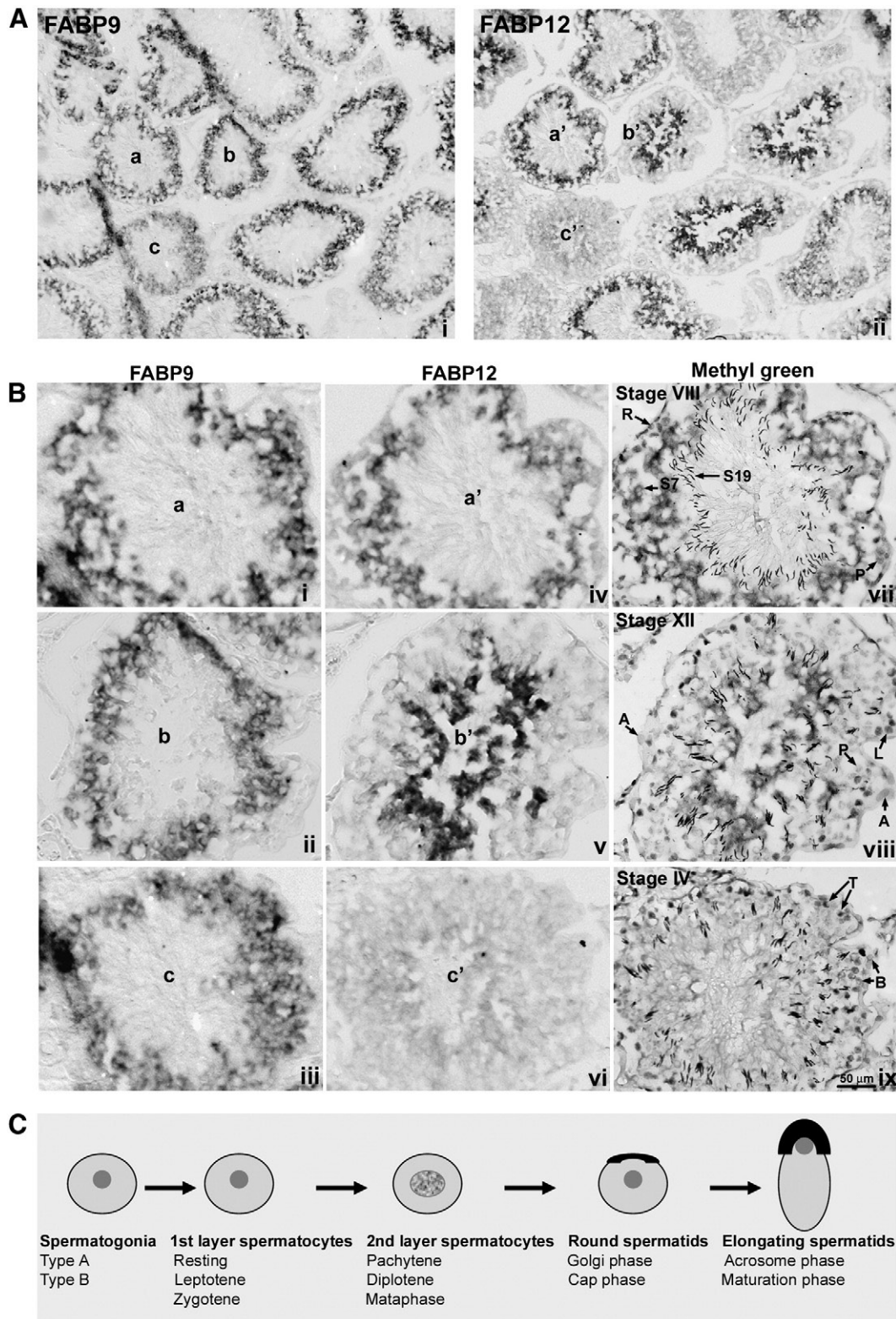


Fig. 8. *FABP9* and *FABP12* mRNA distribution in rat testis. (A) Low magnification view of consecutive tissue sections of adult rat testis hybridized to DIG-11-UTP labeled *FABP9* (Ai) and *FABP12* (Aii) antisense riboprobes. Seminiferous tubules showing distinct *FABP9* (a, b, c) and *FABP12* (a', b', c') hybridization signals are magnified in B. (B) Single seminiferous tubules hybridized to *FABP9* (Bi-iii) or *FABP12* (Biv-vi) riboprobes. *FABP12*-stained seminiferous tubules were counterstained with methyl green in Bvii-ix. Stages of the seminiferous epithelium cycle are defined according to Leblond and Clermont [24,25]. As a negative control, we hybridized consecutive tissue sections with DIG-labeled sense transcripts from either *Fabp12* or *Fabp9*. No signal was observed with either riboprobe (data not shown). (C) Schematic illustration of the developmental stages of germ cells in the testicular seminiferous epithelium. Abbreviations: S7, step 7 spermatids; S19, step 19 spermatids; P, pachytene spermatocytes; R, resting spermatocytes; L, leptotene spermatocytes; A, type A spermatogonia; B, type B spermatogonia; T, transition stage spermatocytes. Scale bar: 50 μ m.

research grant from Alberta Cancer Research Initiative (RG). RZL is the recipient of an Alberta Heritage Foundation for Medical Research fellowship.

Appendix A. Supplementary data

Supplementary data associated with this article can be found, in the online version, at doi:10.1016/j.ygeno.2008.08.003.

References

- [1] D.A. Bernlohr, M.A. Simpson, A.V. Hertz, L.J. Banaszak, Intracellular lipid-binding proteins and their genes, *Annu. Rev. Nutr.* 17 (1997) 277–303.
- [2] J.F. Glatz, G.J. van der Vusse, Cellular fatty acid-binding proteins: their function and physiological significance, *Prog. Lipid. Res.* 35 (1996) 243–282.
- [3] F.G. Schaap, G.J. van der Vusse, J.F. Glatz, Evolution of the family of intracellular lipid binding proteins in vertebrates, *Mol. Cell. Biochem.* 239 (2002) 69–77.
- [4] T. Hanhoff, C. Lucke, F. Spener, Insights into binding of fatty acids by fatty acid binding proteins, *Mol. Cell. Biochem.* 239 (2002) 45–54.
- [5] N.H. Haunerland, F. Spener, Fatty acid-binding proteins—insights from genetic manipulations, *Prog. Lipid. Res.* 43 (2004) 328–349.
- [6] J. Storch, B. Corsico, The emerging functions and mechanisms of mammalian fatty acid-binding proteins, *Annu. Rev. Nutr.* (2008).
- [7] B. Binas, H. Danneberg, J. McWhir, L. Mullins, A.J. Clark, Requirement for the heart-type fatty acid binding protein in cardiac fatty acid utilization, *FASEB J.* 13 (1999) 805–812.
- [8] Y. Owada, S.A. Abdelwahab, N. Kitanaka, H. Sakagami, H. Takano, Y. Sugitani, M. Sugawara, H. Kawashima, Y. Kiso, J.I. Mobarakeh, K. Yanai, K. Kaneko, H. Sasaki, H. Kato, S. Saino-Saito, N. Matsumoto, N. Akaike, T. Noda, H. Kondo, Altered emotional behavioral responses in mice lacking brain-type fatty acid-binding protein gene, *Eur. J. Neurosci.* 24 (2006) 175–187.
- [9] F.G. Schaap, B. Binas, H. Danneberg, G.J. van der Vusse, J.F. Glatz, Impaired long-chain fatty acid utilization by cardiac myocytes isolated from mice lacking the heart-type fatty acid binding protein gene, *Circ. Res.* 85 (1999) 329–337.
- [10] F. Schroeder, A.D. Petrescu, H. Huang, B.P. Atshaves, A.L. McIntosh, G.G. Martin, H. A. Hostetler, A. Vespa, D. Landrock, K.K. Landrock, H.R. Payne, A.B. Kier, Role of fatty acid binding proteins and long chain fatty acids in modulating nuclear receptors and gene transcription, *Lipids* 43 (2008) 1–17.
- [11] J.M. Stewart, The cytoplasmic fatty-acid-binding proteins: thirty years and counting, *Cell. Mol. Life. Sci.* 57 (2000) 1345–1359.
- [12] M. Treuner, C.A. Kozak, D. Gallahan, R. Grosse, T. Muller, Cloning and characterization of the mouse gene encoding mammary-derived growth inhibitor/heart-fatty acid-binding protein, *Gene* 147 (1994) 237–242.
- [13] B. Bleck, C. Hohoff, B. Binas, B. Rustow, C. Dixkens, H. Hameister, T. Borchers, F. Spener, Cloning and chromosomal localisation of the murine epidermal-type fatty acid binding protein gene (Fabpe), *Gene* 215 (1998) 123–130.
- [14] R.Z. Liu, E.M. Denovan-Wright, A. Degraeve, C. Thisse, B. Thisse, J.M. Wright, Differential expression of duplicated genes for brain-type fatty acid-binding proteins (fabp7a and fabp7b) during early development of the CNS in zebrafish (*Danio rerio*), *Gene. Expr. Patterns* 4 (2004) 379–387.
- [15] R.Z. Liu, M.K. Sharma, Q. Sun, C. Thisse, B. Thisse, E.M. Denovan-Wright, J.M. Wright, Retention of the duplicated cellular retinoic acid-binding protein 1 genes (crabp1a and crabp1b) in the zebrafish genome by subfunctionalization of tissue-specific expression, *FEBS J.* 272 (2005) 3561–3571.
- [16] R.Z. Liu, Q. Sun, C. Thisse, B. Thisse, J.M. Wright, E.M. Denovan-Wright, The cellular retinol-binding protein genes are duplicated and differentially transcribed in the developing and adult zebrafish (*Danio rerio*), *Mol. Biol. Evol.* 22 (2005) 469–477.
- [17] M.K. Sharma, V. Saxena, R.Z. Liu, C. Thisse, B. Thisse, E.M. Denovan-Wright, J.M. Wright, Differential expression of the duplicated cellular retinoic acid-binding protein 2 genes (crabp2a and crabp2b) during zebrafish embryonic development, *Gene. Expr. Patterns* 5 (2005) 371–379.
- [18] M.K. Sharma, R.Z. Liu, C. Thisse, B. Thisse, E.M. Denovan-Wright, J.M. Wright, Hierarchical subfunctionalization of fabp1a, fabp1b and fabp10 tissue-specific expression may account for retention of these duplicated genes in the zebrafish (*Danio rerio*) genome, *FEBS J.* 273 (2006) 3216–3229.
- [19] C.H. Schleicher, O.L. Cordoba, J.A. Santome, E.C. Dell'Angelica, Molecular evolution of the multigene family of intracellular lipid-binding proteins, *Biochem. Mol. Biol. Int.* 36 (1995) 1117–1125.
- [20] C. Lucke, L.H. Gutierrez-Gonzalez, J.A. Hamilton, Intracellular lipid binding proteins: evolution, structure, and ligand binding, in: A.K. Duttaroy, F. Spener (Eds.), Cellular proteins and their fatty acids in health and disease, WILEY-VCH Verlag GmbH and Co. KGaA, Weinheim, 2003, pp. 95–118.
- [21] J.D. Thompson, T.J. Gibson, F. Plewniak, F. Jeanmougin, D.G. Higgins, The CLUSTAL_X windows interface: flexible strategies for multiple sequence alignment aided by quality analysis tools, *Nucleic Acids Res.* 25 (1997) 4876–4882.
- [22] R. Breathnach, P. Chambon, Organization and expression of eucaryotic split genes coding for proteins, *Annu. Rev. Biochem.* 50 (1981) 349–383.
- [23] T. Kido, S. Arata, R. Suzuki, T. Hosono, Y. Nakanishi, J. Miyazaki, I. Saito, T. Kuroki, S. Shioda, The testicular fatty acid binding protein PERF15 regulates the fate of germ cells in PERF15 transgenic mice, *Dev. Growth Differ.* 47 (2005) 15–24.
- [24] C.P. Leblond, Y. Clermont, Definition of the stages of the cycle of the seminiferous epithelium in the rat, *Ann. N. Y. Acad. Sci.* 55 (1952) 548–573.
- [25] C.P. Leblond, Y. Clermont, Spermiogenesis of rat, mouse, hamster and guinea pig as revealed by the periodic acid-fuchsin sulfuric acid technique, *Am. J. Anat.* 90 (1952) 167–215.
- [26] F. Ceciliani, H.L. Monaco, S. Ronchi, L. Fatto, P. Spadon, The primary structure of a basic (pI 9.0) fatty acid-binding protein from liver of *Gallus domesticus*, *Comp. Biochem. Physiol. B. Biochem. Mol. Biol.* 109 (1994) 261–271.
- [27] S.M. Di Pietro, E.C. Dell'Angelica, C.H. Schleicher, J.A. Santome, Purification and structural characterization of a fatty acid-binding protein from the liver of the catfish *Rhamdia sapo*, *Comp. Biochem. Physiol. B. Biochem. Mol. Biol.* 113 (1996) 503–509.
- [28] S.M. Di Pietro, J.H. Veerkamp, J.A. Santome, Isolation, amino acid sequence determination and binding properties of two fatty-acid-binding proteins from axolotl (*Ambistoma mexicanum*) liver. Evolutionary relationship, *Eur. J. Biochem.* 259 (1999) 127–134.
- [29] C.H. Schleicher, J.A. Santome, Purification, characterization, and partial amino acid sequencing of an amphibian liver fatty acid binding protein, *Biochem. Cell. Biol.* 74 (1996) 109–115.
- [30] R. Korley, F. Poursmaeili, R. Oko, Analysis of the protein composition of the mouse sperm perinuclear theca and characterization of its major protein constituent, *Biol. Reprod.* 57 (1997) 1426–1432.
- [31] R. Oko, C.R. Morales, A novel testicular protein, with sequence similarities to a family of lipid binding proteins, is a major component of the rat sperm perinuclear theca, *Dev. Biol.* 166 (1994) 235–245.
- [32] J.S. Taylor, I. Braasch, T. Frickey, A. Meyer, Y. Van de Peer, Genome duplication, a trait shared by 22000 species of ray-finned fish, *Genome Res.* 13 (2003) 382–390.
- [33] R.Z. Liu, E.M. Denovan-Wright, J.M. Wright, Structure, linkage mapping and expression of the heart-type fatty acid-binding protein gene (fabp3) from zebrafish (*Danio rerio*), *Eur. J. Biochem.* 270 (2003) 3223–3234.
- [34] R.Z. Liu, V. Saxena, M.K. Sharma, C. Thisse, B. Thisse, E.M. Denovan-Wright, J.M. Wright, The fabp4 gene of zebrafish (*Danio rerio*)—genomic homology with the mammalian FABP4 and divergence from the zebrafish fabp3 in developmental expression, *FEBS J.* 274 (2007) 1621–1633.
- [35] J.P. SanGiovanni, E.Y. Chew, The role of omega-3 long-chain polyunsaturated fatty acids in health and disease of the retina, *Prog. Retin. Eye Res.* 24 (2005) 87–138.
- [36] R. Godbout, H. Marusyk, D. Bisgrove, L. Dabbagh, S. Poppema, Localization of a fatty acid binding protein and its transcript in the developing chick retina, *Exp. Eye Res.* 60 (1995) 645–657.
- [37] T. Helle, S. Deiss, U. Schwarz, B. Schlosshauer, Glial and neuronal regulation of the lipid carrier R-FABP, *Exp. Cell. Res.* 287 (2003) 88–97.
- [38] G.W. Allen, J. Liu, M.A. Kirby, M. De Leon, Induction and axonal localization of epithelial/epidermal fatty acid-binding protein in retinal ganglion cells are associated with axon development and regeneration, *J. Neurosci. Res.* 66 (2001) 396–405.
- [39] R. Godbout, Identification and characterization of transcripts present at elevated levels in the undifferentiated chick retina, *Exp. Eye Res.* 56 (1993) 95–106.
- [40] R.W. Nickells, Ganglion cell death in glaucoma: from mice to men, *Vet. Ophthalmol.* 10 (Suppl 1) (2007) 88–94.
- [41] P. Aoun, J.W. Simpkins, N. Agarwal, Role of PPAR-gamma ligands in neuroprotection against glutamate-induced cytotoxicity in retinal ganglion cells, *Invest. Ophthalmol. Vis. Sci.* 44 (2003) 2999–3004.
- [42] A. Kawasaki, M.H. Han, J.Y. Wei, K. Hirata, Y. Otori, C.J. Barnstable, Protective effect of arachidonic acid on glutamate neurotoxicity in rat retinal ganglion cells, *Invest. Ophthalmol. Vis. Sci.* 43 (2002) 1835–1842.
- [43] M. Ollero, J.G. Alvarez, Fatty acid remodeling during sperm maturation: variation of docosahexaenoic acid content, in: S.R. De Vriese, A.B. Christophe (Eds.), Male Fertility and Lipid Metabolism, The American Oil Chemists Society Press, Urbana, USA, 2003, pp. 23–40.
- [44] G.V. Richieri, R.T. Ogata, A.W. Zimmerman, J.H. Veerkamp, A.M. Kleinfeld, Fatty acid binding proteins from different tissues show distinct patterns of fatty acid interactions, *Biochemistry* 39 (2000) 7197–7204.
- [45] W.M. Grogan, W.F. Farnham, B.A. Szopiak, Long chain polyenoic acid levels in viably sorted, highly enriched mouse testis cells, *Lipids* 16 (1981) 401–410.
- [46] T.N.K.R.B.Q. Tran, Metabolism of long-chain fatty acids in testicular cells, in: C.A. De Vriese SR (Ed.), Male Fertility and Lipid Metabolism, The American Oil Chemists Society Press, Urbana, USA, 2003, pp. 11–22.
- [47] J.E. Parks, D.V. Lynch, Lipid composition and thermotropic phase behavior of boar, bull, stallion, and rooster sperm membranes, *Cryobiology* 29 (1992) 255–266.